Continuous Control Set Model Predictive Control of Buck Converter

Harisyam P V
Electrical Engineering Department
Indian Institute of Science
Bangalore, India
harisyamv@iisc.ac.in

Prasanth V
Texas Instruments
Bangalore, India
prasanth.v@ti.com

Venki Natarajan
Texas Instruments
Bangalore, India
n-venkatesh@ti.com

Kaushik Basu
Electrical Engineering Department
Indian Institute of Science
Bangalore, India
kbasu@iisc.ac.in

***Abstract*—Model Predictive control is a modern method of nonlinear control which gives superior performance with the cost of increased computational burden. In this paper, continuous control set model predictive control (CCS-MPC) for buck converter is proposed. This control strategy achieves constant switching frequency and retains the advantage of faster response of Model predictive control(MPC). The proposed algorithm is based on sampled data model of buck converter. The computation related to solution of a continuous optimization problem is done through a polynomial approximation of a transcendental function. The paper also shows how this approximation is valid for all practically designed buck converters. The proposed control strategy is verified in simulation and compared with experimental results, and it shows good performance for both reference tracking and disturbance rejection. It is superior compared to classical PI with lead controller and is about six times faster than conventional PI with lead controller.**

***Index Terms*—Model Predictive Control, Continuous control set, CCS MPC, Buck converter, fixed switching frequency, Sampled data model**

I. Introduction

Computationally involved Model predictive control (MPC) was common in controlling slow plants in process industries from 1980s. MPC, as its name suggests, predicts future states for the duration of a prediction horizon and applies an optimal input which minimizes a user defined cost function. MPC became attractive because of its faster dynamic response. Computational requirements increase exponentially with prediction horizon [6]. With advancements in microcontrollers and their processing capabilities, it has now become possible to implement computationally complex non-linear control algorithms like MPC in power converters [2]. To minimize computation, the prediction horizon for power converter is chosen to be as minimum as possible, that is one switching period. MPC is broadly classified as Finite Control Set Model Predictive Control (FCS-MPC) and Continuous Control Set Model Predictive Control (CCS-MPC) [6]. [1] discusses about the state of art for FCS-MPC in power electronics applications. [3] and [4] discuss about FCS-MPC with longer prediction horizon for boost converter. FCS-MPC in power electronics has been explored to a greater extent because of its intuitive nature and lower computation cost, but it usually results in variable switching frequency for power converters. In power electronic converters, switching frequency is related to filter design and losses and therefore it is not desired to have switching frequency varying over a wide range. FCS-MPC has also found its path to have a frequency spectrum within a narrow band by including switching frequency in cost function [7]. In recent past, CCS MPC is also being explored, [8] proposed a way to control the output voltage of a buck converter. The response is slow due to the fact that it used approximations in modelling and inductor current is used to control the output voltage.

CCS-MPC comes with the challenge of finding an optimal input from a continuous set of inputs. It is further divided into two types: Generalized predictive control (GPC) and Explicit MPC (EMPC) [6]. The former finds the optimal input by solving optimization problem online and the latter finds it from a look up table. References [11] and [12] discuss explicit MPC algorithm for buck converter, but the development of look up table is an involved process. CCS is better than FCS for DC-DC converters as it results in fixed frequency operation, but is computationally more challenging. This paper proposes a CCS based MPC algorithm for a buck converter. Here the update rate is same as one switching cycle and the prediction horizon is chosen as unity to reduce computational efforts. The control algorithm uses sampled data model to a) estimate the states at the beginning of next state and b) compute the optimal duty cycle to be applied in the next cycle based on sensed values of states in the present cycle. As expected, the optimisation problem needed to find an optimal duty cycle requires solution of a complex transcendental equation to be solved in real time. The paper presents a simple polynomial approximation which is valid for any practical buck converter, that results in a simple closed form solution of the optimal duty cycle. The proposed algorithm is implemented on a hardware and compared with a classical PI with lead controller designed based on averaged model of the buck converter. The proposed controller achieves a six times faster bandwidth.

This paper is organised in six sections. The first section gives an introduction about MPC in power converters. Second section deals with exact modelling of the buck converter, that is sampled data model. MPC algorithm proposed in this paper is discussed in the third section, third chapter also discusses

Texas Instruments - Indian Institute of Science Scholarship Program.

978-1-7281-5414-5/20/$31.00 ©2020 IEEE

algorithm simplification. Fourth section presents state of the art in controlling buck converter, that is frequnecy domain control using state space averaging. Fifth section explains experimental setup and gives simulation as well as experimental results. The sixth section is the conclusion to this paper.

II. Sampled data modelling of buck converter

Buck converter being a second order system, has two states, inductor current and capacitor voltage. Switching time period, T_s is the duration of a switching cycle or inverse of switching frequency (f_s). Given the states at the beginning of a switching cycle and the duty ratio that is going to be applied in that switching cycle, states at the end of that switching cycle can be computed.

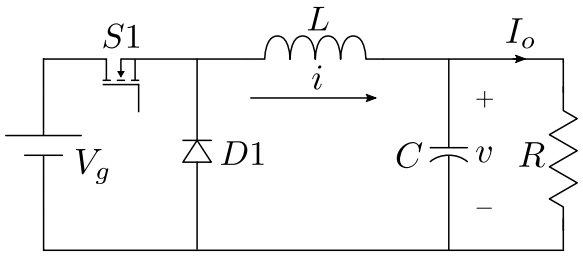

Fig. 1: Buck converter

Fig. 1 shows the circuit diagram of a buck converter. Switch $S1$ is on for an initial duration of dT_s in every switching cycle, where d is the duty ratio. The equivalent circuit during this period is as given in Fig. 2. For the remaining duration of $(1-d)T_s$ in every switching cycle, $S1$ is off and $D1$ conducts (shown in Fig. 3). Thus the buck converter switches between two linear circuits within every switching cycle.

We are interested in finding the values of state variables, at the start of every switching cycle, $x[k]$, where argument k represents k^{th} cycle. In order to find $x[k+1]$, we first need to find the intermediate states $x[k+d]$, states at the end of on-state. This is used to find states at start of the next switching cycle, $x[k+1]$. Arguments are summarised below:

- $k \rightarrow$ start of current switching cycle
- $k+d \rightarrow$ end of on-state in current switching cycle
- $k+1 \rightarrow$ end of current cycle / start of next cycle

A. Buck converter in on-state

Differential equations governing the circuit in Fig.2 are given in (1). This is solved for a duration of dT_s, and states at the end of on-state can be written as functions of states at the start of the switching cycle and the input voltage, which is given in (2). Matrices A_{on} and B_{on} are functions of L, C, R and T_s.

$$\begin{bmatrix} di/dt \\ dv/dt \end{bmatrix} = \begin{bmatrix} 0 & -1/L \\ 1/C & -1/RC \end{bmatrix} \begin{bmatrix} i \\ v \end{bmatrix} + \begin{bmatrix} 1/L \\ 0 \end{bmatrix} V_g \tag{1}$$

$$\begin{bmatrix} i[k+d] \\ v[k+d] \end{bmatrix} = A_{on} \begin{bmatrix} i[k] \\ v[k] \end{bmatrix} + B_{on} V_g \tag{2}$$

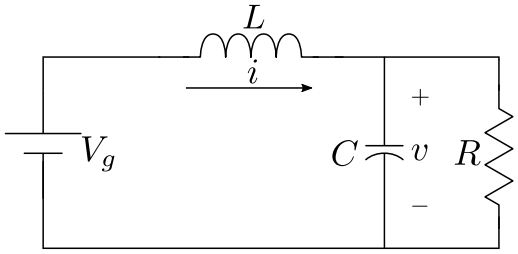

Fig. 2: Buck converter in on-state ($kTs \leq t < (k+d)Ts$)

B. Buck converter in off-state

Differential equations governing the circuit in Fig.3 are given in (3). This is solved for a duration of $(1-d)T_s$, and state variables at the end of the switching cycle can be written as functions of states at the end of on-state, which is given in (4). Elements of matrix A_{off} are functions of L, C, R and T_s.

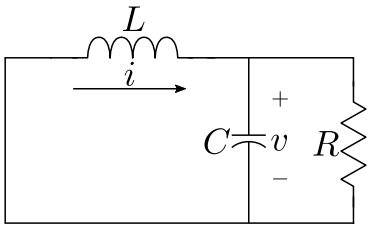

Fig. 3: Buck converter in off-state ($(k+d)Ts \leq t < (k+1)Ts$)

$$\begin{bmatrix} di/dt \\ dv/dt \end{bmatrix} = \begin{bmatrix} 0 & -1/L \\ 1/C & -1/RC \end{bmatrix} \begin{bmatrix} i \\ v \end{bmatrix} \tag{3}$$

$$\begin{bmatrix} i[k+1] \\ v[k+1] \end{bmatrix} = A_{off} \begin{bmatrix} i[k+d] \\ v[k+d] \end{bmatrix} \tag{4}$$

Substituting (2) in (4), the sampled data model of buck converter can be written, which expresses states at the end of a switching cycle as functions of states at the beginning of that cycle and input voltage, as given in (5). Since the RLC network does not change for the entire duration of the switching period, it is noted that the elements in state matrix A, B, C *and* D are independent of d, and only the elements in input matrix $E_1(d)$ and $F_1(d)$ depend on d. The term d is embedded in these terms as part of exponential and sinusoidal functions.

$$\begin{bmatrix} i[k+1] \\ v[k+1] \end{bmatrix} = \begin{bmatrix} A & B \\ C & D \end{bmatrix} \begin{bmatrix} i[k] \\ v[k] \end{bmatrix} + \begin{bmatrix} E_0 + E_1(d) \\ F_0 + F_1(d) \end{bmatrix} V_g \tag{5}$$

The state space representation of the sampled data model is written in a compact way by introducing the following variables: base resistance $R_0 = \sqrt{L/C}$, per unit angular frequency $\omega = T_s/\sqrt{LC}$, damping ratio $\zeta = R_0/2R$ and d' is defined as $1-d$. Based on whether the system is over-damped($\zeta > 1$) or under-damped($\zeta < 1$), elements of state and input matrix in (5) have different expressions. Few more terms are introduced for over-damped case, $\zeta' = \sqrt{\zeta^2 - 1}$, $s_1 = \omega(-\zeta + \zeta')$ and $s_2 = \omega(-\zeta - \zeta')$.

Elements in the state matrix for $\zeta < 1$:

$$A = \exp(-\omega\zeta)\left\{\frac{\zeta}{\sqrt{1-\zeta^2}}\sin(\omega\sqrt{1-\zeta^2}) + \cos(\omega\sqrt{1-\zeta^2})\right\} \quad (6)$$

$$B = \frac{\exp(-\omega\zeta)}{R}\left\{\frac{\sin(\omega\sqrt{1-\zeta^2})}{2\zeta\sqrt{1-\zeta^2}}\right\} \quad (7)$$

$$C = \exp(-\omega\zeta)\left\{\frac{2\zeta}{\sqrt{1-\zeta^2}}\sin(\omega\sqrt{1-\zeta^2})\right\}R \quad (8)$$

$$D = \exp(-\omega\zeta)\left\{\cos(\omega\sqrt{1-\zeta^2}) - \frac{\zeta}{\sqrt{1-\zeta^2}}\sin(\omega\sqrt{1-\zeta^2})\right\} \quad (9)$$

Elements in the state matrix for $\zeta > 1$:

$$A = \left\{\frac{1}{2\zeta'}\right\}\{(\zeta+\zeta') * e^{s_1} + (-\zeta+\zeta') * e^{s_2}\} \quad (10)$$

$$B = \left\{\frac{1}{4R\zeta\zeta'}\right\}\{-e^{s_1} + e^{s_2}\} \quad (11)$$

$$C = \left\{\frac{R\zeta}{\zeta'}\right\}\{e^{s_1} - e^{s_2}\} \quad (12)$$

$$D = \left\{\frac{1}{2\zeta'}\right\}\left\{(-\zeta+\zeta') * e^{s_1} + (\zeta+\zeta') * e^{s_2)}\right\} \quad (13)$$

$$E^{\zeta<1} = \underbrace{\frac{-\exp(-\omega\zeta)}{R}\left\{\cos(\omega\sqrt{1-\zeta^2}) + \frac{2\zeta^2-1}{2\zeta\sqrt{1-\zeta^2}}\sin(\omega\sqrt{1-\zeta^2})\right\}}_{E_0} + \underbrace{\frac{\exp(-\omega\zeta d')}{R}\left\{\cos(\omega d'\sqrt{1-\zeta^2}) + \frac{2\zeta^2-1}{2\zeta\sqrt{1-\zeta^2}}\sin(\omega d'\sqrt{1-\zeta^2})\right\}}_{E_1(d)} \quad (14)$$

$$F^{\zeta<1} = \underbrace{-\exp(-\omega\zeta)\left\{\cos(\omega\sqrt{1-\zeta^2}) + \frac{\zeta}{\sqrt{1-\zeta^2}}\sin(\omega\sqrt{1-\zeta^2})\right\}}_{F_0} + \underbrace{\exp(-\omega\zeta d')\left\{\cos(\omega d'\sqrt{1-\zeta^2}) + \frac{\zeta}{\sqrt{1-\zeta^2}}\sin(\omega d'\sqrt{1-\zeta^2})\right\}}_{F_1(d)} \quad (15)$$

$$E^{\zeta>1} = \underbrace{\left\{\frac{\zeta+\zeta'-(\zeta+\zeta')^3}{8R\zeta\zeta'}e^{s_1} + \frac{\zeta-\zeta'-(\zeta-\zeta')^3}{8R\zeta\zeta'}e^{s_2}\right\}}_{E_0} + \underbrace{\left\{\frac{2\zeta^2+2\zeta\zeta'-1}{4R\zeta\zeta'}e^{(s_1d')} + \frac{-2\zeta^2+2\zeta\zeta'+1}{4R\zeta\zeta'}e^{(s_2d')}\right\}}_{E_1(d)} \quad (16)$$

$$F^{\zeta>1} = \underbrace{\left\{\frac{(1-(\zeta+\zeta')^2)}{4\zeta'}e^{s_1} + \frac{(1-(-\zeta+\zeta')^2)}{4\zeta'}e^{s_2}\right\}}_{F_0} + \underbrace{\left\{\frac{\zeta+\zeta'}{2\zeta'}e^{(s_1d')} + \frac{-\zeta+\zeta'}{2\zeta'}e^{(s_2d')}\right\}}_{F_1(d)} \quad (17)$$

III. Model Predictive control for buck converter

The control objective is to maintain the output voltage to a reference value. The control input that can be applied to the converter is duty-ratio d. There exists only one input d, in a switching period and therefore, optimal d has to be computed and applied once in every switching period. Practical controllers take a finite time for computation, and hence there is a delay in applying the input d. This time delay can be compensated by computing states of the next sampling interval using the sampled data model, [5]. The duty cycle value which is computed in the present switching cycle is implemented only in the next cycle. In this paper, CCS-MPC algorithm is proposed and is compared with the conventional PI with lead compensator for buck converter. Time delay compensation is also achieved in the proposed strategy.

A. MPC Algorithm

In this strategy, the output voltage is controlled by minimizing error, that is, the difference between the estimated output voltage and reference value. The duty ratio that is going to be applied in every k^{th} sampling interval is already decided in the previous step. What can be decided in k^{th} sampling interval is d_{k+1}, to be applied in next interval $(k+1)$. This is because practical computation takes time. The states at $(k+1)^{th}$ interval $(i[k+1], v[k+1])$ are independent of the computations performed in the k^{th} interval and depend only on d_k. Estimated states $(i^e[k+1], v^e[k+1])$ are computed in k^{th} interval using measured values of $i[k], v[k]$ and d_k computed in previous cycle. Optimal input in $(k+1)^{th}$ interval will be the one which minimizes error at $(k+2)^{th}$ interval. This requires information about states at $(k+1)^{th}$ interval in k^{th} interval, which can be computed from the sampled data model.

Therefore, in the first step, delay compensation is achieved by estimating states at $(k+1)^{th}$ sampling interval. This is done by using input (d_k) and the sensed values of states ($i[k]$ and $v[k]$) at the start of k^{th} cycle in the sampled data model of the converter. Then, in the next step, optimal input at $(k+1)^{th}$ sampling interval is computed by minimizing the error in $(k+2)^{th}$ sampling interval. This algorithm is shown in Fig. 4.

Using (5), the states at $(k+1)^{th}$ instant, $i^e[k+1]$ and $v^e[k+1]$ can be estimated, given $i[k]$, $v[k]$ and d_k. Now, with sampled data model, the output voltage at $(k+2)^{th}$ instant can be estimated as a function of d_{k+1} and the estimated states at $(k+1)^{th}$ interval (as given in (18)). From this, the optimal

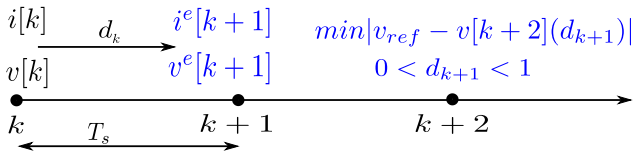

Fig. 4: MPC problem formulation for buck converter

input, d_{k+1} which minimizes the error has to be computed.

$$v[k+2](d_{k+1}) = Ci^e[k+1] + Dv^e[k+1] + \Big(F_0 + F_1(d_{k+1})\Big)V_g \quad (18)$$

A closer look at (18), using previously found expressions for F_0 and F_1 (from (15) and (17)) reveals that $v[k+2](d_{k+1})$ is a monotonic function of d_{k+1}. It could be anywhere between v^{min}_{k+2} (when $d_{k+1} = 0$) and v^{max}_{k+2} (when $d_{k+1} = 1$). Now there are three cases. First case, if v_{ref} is less than or equal to v^{min}_{k+2} then $d^{opt}_{k+1} = 0$ is applied. Second case, if v_{ref} is greater than or equal to v^{max}_{k+2} then $d^{opt}_{k+1} = 1$ is applied and in third case case, if v_{ref} is in between v^{min}_{k+2} and v^{max}_{k+2}, then duty ratio d^{opt}_{k+1} is found which makes $v[k+2](d_{k+1}) = v_{ref}$. This is shown in Fig. 5.

$$d^{opt}_{k+1} = \begin{cases} 0, & v_{ref} \le v^{min}_{k+2} \\ 1, & v_{ref} \ge v^{max}_{k+2} \\ \text{solve } v_{ref} - v[k+2](d_{k+1}) = 0, & \text{otherwise} \end{cases} \quad (19)$$

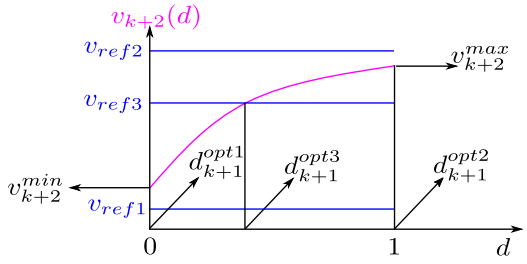

Fig. 5: Graphical representation to find optimal input d^{opt}_{k+2} a)$v_{ref} \le v^{min}_{k+2}$ b)$v_{ref} \ge v^{max}_{k+2}$ c)$v^{min}_{k+2} < v_{ref} < v^{max}_{k+2}$

When $v^{min}(k+2) < v_{ref} < v^{max}(k+2)$, determination of d^{opt}_{k+1} requires finding solution of a transcendental equation, which is difficult to accomplish in real time computation on a microcontroller. There arises a need for the replacement of complex exponential and trigonometric functions so that they are solvable online. Polynomial approximation of (15) and (17) can be used to find an optimal input if it satisfies certain conditions. It can be applied to exponential and sinusoidal expressions if their arguments are less than 1. This is analysed in this paper. Arguments of exponential and sinusoidal functions present in (15) and (17) are listed below in Table I:

TABLE I: Arguments of exponential and sinusiodal functions

Under-damped RLC	Over-damped RLC
$-\zeta\omega d'$	$\omega d'(-\zeta + \zeta')$
$\omega d'\sqrt{1-\zeta^2}$	$\omega d'(-\zeta - \zeta')$

In all practical designs of the buck converter, LC corner frequency is chosen to be less than the switching frequency. The peak to peak ripple in output voltage for the buck converter is given below, where $\bar{v}$ is the average output voltage and Δv represents the peak to peak ripple in output voltage. ω can be expressed as a function of the design specification from (21) as given in (22). Output voltage ripple in practical designs tends to have a small value, the ratio $\Delta v/\bar{v}$ is usually lower than 0.02. Therefore ω tends to be of a small magnitude, much less than 1.

$$\bar{v} = dV_g \quad (20)$$

$$\frac{\Delta v}{\bar{v}} = \frac{(1-d)T_s^2}{8LC} \quad (21)$$

$$\omega = \sqrt{\left(\frac{8}{1-d}\right)\left(\frac{\Delta v}{\bar{v}}\right)} \quad (22)$$

Also from the equation for peak to peak ripple in inductor current as given in (23), it is observed that the value of ζ is not very large, though it can be greater than 1. It is because a higher value of ζ will correspond to tighter inductor current ripple criteria, and hence very large value of inductance. Δi and I_o in (23) and (24) correspond to peak to peak ripple in inductor current and average load current ($\bar{v}/R$) respectively. ζ can be expressed as a function of the design specification from (23) as given in (24).

$$\frac{\Delta i}{I_o} = \frac{R(1-d)T_s}{L} \quad (23)$$

$$\zeta = \frac{(1-d)\omega}{2\ (\Delta i/I_o)} \quad (24)$$

From Table I, every argument is a product of ω, d' and a function of damping factor ζ. Now, ω and d' are smaller than 1. For under-damped case, ζ and $\sqrt{1-\zeta^2}$ are having magnitudes less than 1. So it is clear that for under-damped case the argument will be much smaller than 1. For over-damped case $\zeta > 1$, but from the previous discussion ζ and hence ζ' will not be large in magnitude, thus making the arguments smaller than 1.

Therefore, in almost all practical designs, arguments are less than 1. With this, polynomial approximation for exponential and sinusoidal functions is used to solve minimization problem given in (19). Polynomial approximation up to second order is considered since there is no linear term. This is shown in (25), it is also noted that the expression for $F_1(d)$ remains the same for both under-damped and over-damped conditions.

$$F_1(d) \approx 1 - \frac{(\omega(1-d))^2}{2} \quad (25)$$

This expression for $F_1(d)$ is used to solve (19) to find out optimal duty ratio, d_{k+1}. Since (19) is a quadratic equation, it has two solutions. However, there is only one valid solution for it since $F_1(d)$ is a monotonic function of d. The valid one which lies within the range $(0, 1)$ is the smaller root which is obtained by taking positive square root in quadratic formula.

IV. Classical control of buck converter

A classical PI with lead controller is designed for the buck converter to compare its performance with MPC controller. The plant transfer function is derived from averaged model of the converter [10]. Based on averaging over a switching cycle, plant transfer function is derived as given in (27). For the buck converter designed for experiment, parameters are given in Table II.

$$G(s) = \frac{\bar{v}(s)}{d(s)} = \frac{Vg/(LC)}{s^2 + s/(RC) + 1/(LC)} \tag{26}$$

$$= \frac{2.366 * 10^9}{s^2 + 7922s + 8.45 * 10^7} \tag{27}$$

PI with lead controller is designed with a phase margin of 60^o and a bandwidth of $2kHz$, which is one tenth of the switching frequency. PI with lead controller transfer function is given below in (28). Bode plot of loop gain transfer function is shown in Fig. 6.

$$C(s) = \frac{50\left(1 + \frac{s}{2000}\right)\left(1 + \frac{s}{6000}\right)}{s\left(1 + \frac{s}{60000}\right)} \tag{28}$$

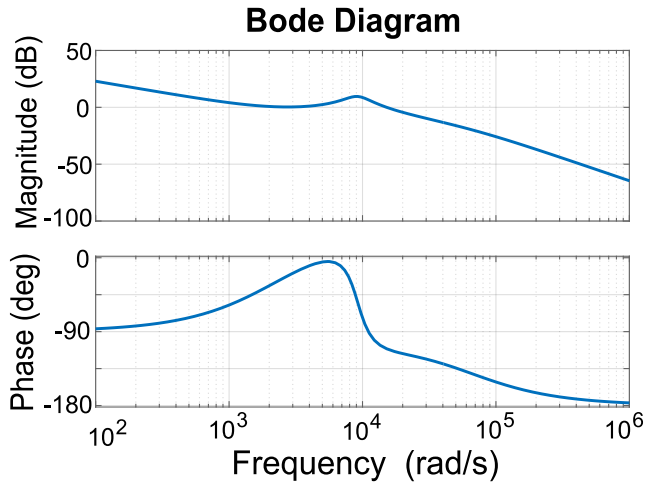

Fig. 6: Bode plot of loop gain G(s)C(s)

V. Simulation and Experimental Results

A. Experimental setup

Texas Instruments' microcontroller $TMS320F28379D$ (Delfino) is used to control the buck converter. Experimental setup for buck converter and controller is shown in Fig. 7 and parameter values are given in Table II. It includes Buck converter hardware and microcontroller launchpad. $IR2100$ gate driver IC is used to drive $IRF840$ mosfet and body diode of $IRF840$ is used in place of diode in the converter. The states, inductor current and output voltage after signal conditioning, are passed to ADC of the microcontroller. Computation is done in the microcontroller and it generates PWM signal corresponding to MPC algorithm. This signal is then passed to gate driver of the mosfet in buck converter.

TABLE II: Parameters

Input Voltage (V_g)	$30V$
Filter Inductance (L)	$330\mu H$
Filter Capacitor (C)	$47\mu F$
Load Resistance (R)	7.5Ω
Switching frequency (f_s)	$20kHz$
Update period (T_s)	$50\mu s$

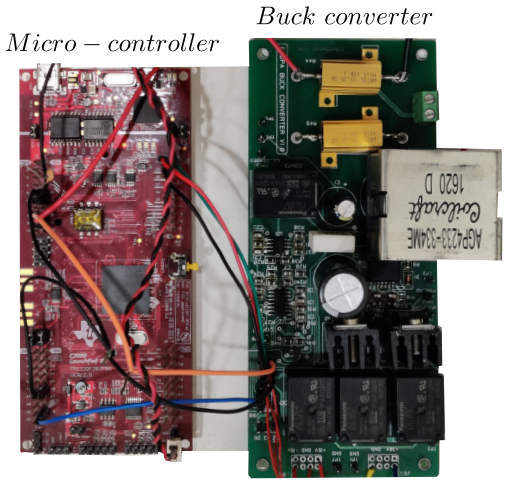

Fig. 7: Experimental set up

B. Results

MPC algorithm shown in Fig. 4 is verified in simulation and experiment, and compared with PI with lead controller. Simulation is done in MATLAB Simulink. Analysis is done for performance of disturbance rejection (load change) and step change in reference voltage. Fig. 8, 9 and 10 shows that simulation and experimental results are matching. This validates both experiment and simulation.

In first case, there is load reduction from 7.5Ω to 15Ω given in Fig. 8 and in next case, there is loading from 15Ω to 7.5Ω given in Fig. 9. It is observed that MPC controller corrected back to reference value within about 5 to 6 switching cycles or $300\mu s$.This verifies the high speed transient response of MPC controller which also maintains good steady state response.

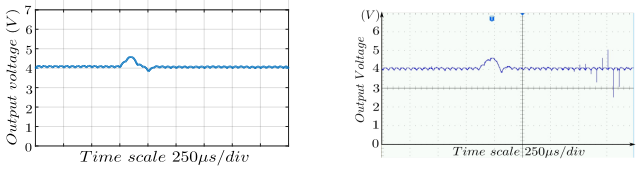

(a) Simulation (b) Experimental Results

Fig. 8: Response for a load change from 7.5Ω to$15\ \Omega$

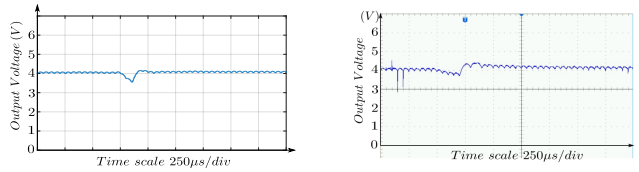

(a) Simulation (b) Experimental Results

Fig. 9: Response for a load change from 15Ω to 7.5Ω

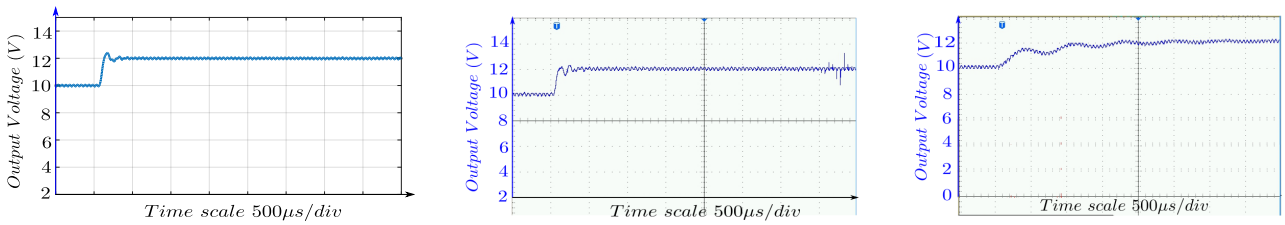

(a) MPC Simulation (b) MPC Experimental (c) PI with lead controller

Fig. 10: Response for a step change in reference from 10V to 12V

The reference voltage is changed from 10V to 12V and the results are shown in Fig. 10. The controller corrected the output voltage to the new reference value within 8 to 10 switching cycles or 500μs. It is inferred that the proposed MPC algorithm has a superior dynamic performance compared to classical PI with lead controller in terms of the speed of response. For a step change in reference voltage from 10V to 12V, the response of PI with lead controller settled within 3ms, which is around six times that of the MPC controller.

These advantages, however, come with the cost of an increased computational burden for MPC control. Microcontroller TMS320F28379D was used with a clock frequency of 100MHz to compare control strategies. Computation time for MPC algorithm was 12.5μs, whereas in PI with lead controller, the computation time was only 1.35μs. The proposed strategy also has other limitations, it does not control or limit the state inductor current and requires sensing of load current to estimate load resistance R.

VI. Conclusion

In this paper a continuous control set based model predictive control (CCS MPC) strategy is developed for controlling the output voltage of a buck converter operating in continuous conduction mode. The prediction horizon is chosen to be unity with the update rate same as switching frequency. This strategy employs the sample data model of buck converter based on exact solution of circuit dynamics. Plant variations because of load change was accounted by sensing the load current and estimating load resistance. The proposed strategy takes care of one cycle delay in application of the optimal duty cycle, due to finite computation time required to determine its value by the microcontroller. Determination of optimal duty ratio required solution of a transcendental equation. The paper found an approximate closed form expression of the optimal duty cycle, so that the computationally intensive solution of the transcendental equation can be avoided. This approximation is valid for all well designed buck converter. The controller could correct error within few switching cycles. Both simulation and experimental results show that the proposed controller achieves almost six times faster error correction rate when compared with a classical controller (PI with lead). Steady state performance of the controller is similar to conventional controller maintaining a constant duty ratio without any limit cycle oscillations. It is also shown experimentally that with the present day high performance micro-controllers, it is possible to implement this computationally involved algorithm quite effectively. The computation time for proposed algorithm was about ten times than that of the PI with lead controller, indicating its computational complexity.

References

[1] J. Rodriguez et al., "State of the Art of Finite Control Set Model Predictive Control in Power Electronics," in IEEE Transactions on Industrial Informatics, vol. 9, no. 2, pp. 1003-1016, May 2013. doi: 10.1109/TII.2012.2221469

[2] S. Kouro, P. Cortes, R. Vargas, U. Ammann and J. Rodriguez, "Model Predictive Control—A Simple and Powerful Method to Control Power Converters," in IEEE Transactions on Industrial Electronics, vol. 56, no. 6, pp. 1826-1838, June 2009. doi: 10.1109/TIE.2008.2008349.

[3] P. Karamanakos, T. Geyer and S. Manias, "Direct Voltage Control of DC–DC Boost Converters Using Enumeration-Based Model Predictive Control," in IEEE Transactions on Power Electronics, vol. 29, no. 2, pp. 968-978, Feb. 2014. doi: 10.1109/TPEL.2013.2256370.

[4] P. Karamanakos, T. Geyer and S. Manias, "Direct voltage control of DC-DC boost converters using model predictive control based on enumeration," 2012 15th International Power Electronics and Motion Control Conference (EPE/PEMC), Novi Sad, 2012, pp. DS2c.10-1-DS2c.10-8. doi: 10.1109/EPEPEMC.2012.6397293.

[5] P. Cortes, J. Rodriguez, C. Silva and A. Flores, "Delay Compensation in Model Predictive Current Control of a Three-Phase Inverter," in IEEE Transactions on Industrial Electronics, vol. 59, no. 2, pp. 1323-1325, Feb. 2012. doi: 10.1109/TIE.2011.2157284.

[6] S. Vazquez, J. Rodriguez, M. Rivera, L. G. Franquelo and M. Norambuena, "Model Predictive Control for Power Converters and Drives: Advances and Trends," in IEEE Transactions on Industrial Electronics, vol. 64, no. 2, pp. 935-947, Feb. 2017. doi: 10.1109/TIE.2016.2625238.

[7] M. Aguirre, S. Kouro, C. A. Rojas and S. Vazquez, "Enhanced Switching Frequency Control in FCS-MPC for Power Converters," in IEEE Transactions on Industrial Electronics. doi: 10.1109/TIE.2020.2973907

[8] Z. Leng and Q. Liu, "A simple model predictive control for Buck converter operating in CCM," 2017 IEEE International Symposium on Predictive Control of Electrical Drives and Power Electronics (PRECEDE), Pilsen, 2017, pp. 19-24.

[9] F. Donoso, A. Mora, R. Cárdenas, A. Angulo, D. Sáez and M. Rivera, "Finite-Set Model-Predictive Control Strategies for a 3L-NPC Inverter Operating With Fixed Switching Frequency," in IEEE Transactions on Industrial Electronics, vol. 65, no. 5, pp. 3954-3965, May 2018.

[10] R. W. Erickson and D. Maksimovic, Fundamentals of Power Electronics, 2ed ed. Springer, 2001.

[11] C. Vlad, P. Rodriguez-Ayerbe, E. Godoy and P. Lefranc, "Explicit model predictive control of buck converter," 2012 15th International Power Electronics and Motion Control Conference (EPE/PEMC), Novi Sad, 2012, pp. DS1e.4-1-DS1e.4-6, doi: 10.1109/EPEPEMC.2012.6397240.

[12] S. Mariethoz, A. G. Beccuti, G. Papafotiou and M. Morari, "Sensorless explicit model predictive control of the DC-DC buck converter with inductor current limitation," 2008 Twenty-Third Annual IEEE Applied Power Electronics Conference and Exposition, Austin, TX, 2008, pp. 1710-1715, doi: 10.1109/APEC.2008.4522957.

[13] X. Zhang, B. Wang, U. Manandhar, H. Beng Gooi and G. Foo, "A Model Predictive Current Controlled Bidirectional Three-Level DC/DC Converter for Hybrid Energy Storage System in DC Microgrids," in IEEE Transactions on Power Electronics, vol. 34, no. 5, pp. 4025-4030, May 2019, doi: 10.1109/TPEL.2018.2873765.